

Analysis of anaerobic digester mixing: comparison of long shafted paddle mixing vs gas mixing

U. Bergamo, G. Viccione , S. Coppola, A. Landi, A. Meda and C. Gualtieri

ABSTRACT

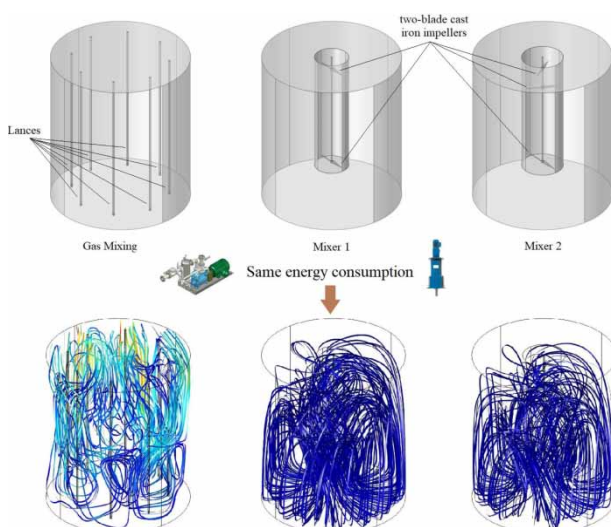
The anaerobic digestion (AD) process is influenced by a variety of operation parameters, such as sludge rheology, mixing, temperature, solid retention time (SRT), hydraulic retention time (HRT) and solids concentration. The optimum in the mixing lies somewhere between no-mixing and continuous mixing, as the lack or excessive mixing can lead to poor AD performance instead. A three-dimensional computational fluid dynamics steady/unsteady model, incorporating the rheological properties of the sludge, was developed and applied to quantify mixing in a full-scale anaerobic digester. Mechanical and gas mixing solutions were taken into account, keeping constant the daily energy consumption. Results, consisting of velocity magnitude and patterns, dead zone formation and turbulence levels were discussed. Compared to the mechanical mixing, gas mixing had lower percentage of dead zones (about 5% against 50%), larger maximum velocity (about 3 m/s against 1 m/s) as well as larger turbulent kinetic energy levels ($0.24 \text{ m}^2/\text{s}^2$ against $0.001 \text{ m}^2/\text{s}^2$).

Key words | anaerobic digester, biogas, CFD, gas mixing, mechanical mixing, sludge rheology


HIGHLIGHTS

- Mechanically stirred and gas-mixed anaerobic digestion solutions were compared.
- Daily energy consumption ($E = 140.4 \text{ kWh}$) was kept constant.
- Detailed CFD modelling for non-Newtonian sludge in full-scale anaerobic digesters.
- Flow patterns, dead zones and turbulence levels were compared and discussed.
- Gas mixing yielded better results in terms of velocities, dead zones and turbulence levels.

GRAPHICAL ABSTRACT



doi: 10.2166/wst.2020.248

U. Bergamo
G. Viccione  (corresponding author)
S. Coppola
 Department of Civil Engineering,
 University of Salerno,
 via Giovanni Paolo II, 132, 84084 Fisciano,
 Italy
 E-mail: gviccion@unisa.it

A. Landi
 MEA S.R.L.,
 Foro Buonaparte, 70, 20121, Milano,
 Italy

A. Meda
 BHU Umwelttechnik GmbH,
 Einsteinstrasse 57, 70229 Leonberg,
 Germany

C. Gualtieri
 Department of Civil, Architectural and
 Environmental Engineering,
 University of Naples Federico II,
 via Claudio, 21, 80125 Naples,
 Italy

INTRODUCTION

Anaerobic digestion is one of the most long-established processes for the stabilization of sewage sludge (Tchobanoglous *et al.* 2014). It is widely used to convert waste into valuable end products such as biogas (Lisowij & Wright 2020). A number of advantages can be ascribed to the use of anaerobic digestion. First of all, it is a source of renewable energy, replacing fossil fuels, such as gas petrol liquid for cooking included as well as allowing a reduction of gas emissions into the atmosphere from landfilling sites (Angelidaki *et al.* 2003). Anaerobic digestion can be employed to treat landfill leachate (Abuabdou *et al.* 2018, 2020), a highly contaminated wastewater which when accidentally released into the environment poses a severe threat for aquifers, aquatic ecosystems and human health (Stoppiello *et al.* 2020). Digesters in wastewater treatment plants to treat sewage sludge consist of insulated concrete or steel structures, usually cylindrical or egg-shaped, with a conical bottom from which the digested sludge is extracted. Recently, a renewed interest in anaerobic digesters has appeared (Kariyama *et al.* 2018; Sadino-Riquelme *et al.* 2018; Wang *et al.* 2018). Factors such as sewage sludge disposal and the pursuit of climate protection objectives gave reason to re-think the classical, long established approaches concerning wastewater and sludge treatment for sewage treatment plants, even in the case of small to medium size (approximately 5,000 to 50,000 population equivalent). In Germany, for instance, MULEWF (2014) and DWA (2015) reports proved that it is profitable to implement an anaerobic sludge digestion with biogas utilization in a co-generation unit for plant of small size against the common practice of aerobic simultaneous sludge stabilization. This new trend is giving a boost to the implementation of the anaerobic sludge digestion technology (Zare *et al.* 2019).

The anaerobic digestion process is sensitive to a large number of factors: temperature, retention time, nutrients concentration, pH and inhibitors concentration, mixing type and intensity (Dapelo 2016). Temperature is a main factor affecting the process. Appels *et al.* (2008) recommended temperature variation within 0.6 °C per day. Solid (SRT) and hydraulic (HRT) retention times are important parameters as well, depending on geometry, flow rate, and recirculation system. The former indicates the average time that solids, and the bacteria living on them, spend inside the digester, while the latter refers to the liquid fraction. Despite biomass retention being recognised among

the most important parameters of anaerobic digestion providing SRT for the methanogens, poor biomass retention in the conventional anaerobic digesters is often found (Lin *et al.* 2013; Shi *et al.* 2017). The pH is a key parameter related to the efficient running of a digester. Most fermentative bacteria can thrive in a wide range of pH, between 4.0 and 8.5, but their by-products depend on pH (Dapelo 2016).

Effective anaerobic digestion is highly dependent on mixing system and frequency as well (Subramanian *et al.* 2015; Wang *et al.* 2019). As defined in the *Handbook of Industrial Mixing: Science and Practice* (Paul *et al.* 2004), mixing is 'the reduction of inhomogeneity in order to achieve a desired process result. The inhomogeneity can be one of concentration, phase, or temperature. Secondary effects, such as mass transfer, reaction, and product properties are usually the critical objectives'. Therefore, mixing promotes the establishment of a homogeneous environment for anaerobic digestion, by reducing temperature, concentration and other field gradients inside the reactor (Appels *et al.* 2008; Sindall *et al.* 2013). Meegoda *et al.* (2018) provided a comprehensive list of issues related to digester mixing.

Solid settling, short-circuiting, dead-zone, and scum formation arising from poor mixing are still major problems leading to less than optimal biogas production. Borole *et al.* (2006) proved that a pilot-scale digester with dairy manure yields continuous methane production with mixing, which soon deteriorates without agitation. On the other hand, the literature shows contributions where biogas production is sustained in unmixed conditions (Ghaly 1989; Wang *et al.* 2019). Similarly, intermittent mixing is sometimes recommended (Lindmark *et al.* 2014; Leite *et al.* 2017). In fact, resting times can result in higher methane yield compared to continuous mixing while avoiding floating layer formation. The reason behind higher gas production is related to a balance reaching among microorganisms involved in the anaerobic conversion of biomass to methane. In addition, intermittent mixing is preferred to save energy compared with continuous mixing solutions (Singh *et al.* 2020). In addition, intermittent mixing results in lower power consumption and maintenance costs related to mixing solutions where two or more digesters are installed in parallel. In this case, it is possible to use one single biogas compressor, shared by the digesters, feeding the units alternately with biogas. On the contrary, continuous mixing requires several compressor units

(usually one per digester) or a larger common compressor unit with a distribution and regulation system for biogas flow splitting. Comprehensive reviews of mixing in anaerobic digesters are given in [Lindmark *et al.* 2014](#); [Kariyama *et al.* 2018](#); and [Singh *et al.* 2019](#).

There are three main mixing methods generally adopted in large-scale application of AD: mechanical mixing, gas mixing and pumped liquid recirculation through externally installed pumps or submerged jets ([Qasim 1999](#)).

Mechanical stirring ([Manea & Robescu 2012](#)) can be done using: (1) low-speed with large impellers (one to three levels) without draft tube, installed on the digester roof; (2) high speed, vertical mixers with one small impeller with draft tube, installed on the digester roof; (3) high speed, inclined mixers with one small impeller installed through the digester wall. In all cases, the rotating impellers displace the sludge, mixing the digester contents. Low-speed turbines usually have one cover-mounted motor with two turbine impellers located at different sludge depths. Biogas production is affected by impeller design, eccentricity, bottom and inter impeller clearance, baffles and position of draft tube. Incorrect choice of impellers and operating speed can lead to ineffective mixing. [Singh *et al.* \(2019\)](#) reported that the geometry of the impeller has a significant effect on digester performance. The impeller should be chosen considering sludge rheology and turbulence to achieve an optimum design ([Wu 2010](#); [Lindmark *et al.* 2014](#); [Torotwa & Ji 2018](#)).

In gas mixing systems ([Chandran *et al.* 2017](#); [Serna-Maza *et al.* 2017](#)), gas recirculation inside the digester acts as mixer. They can be unconfined or confined: the former are designed to collect biogas at the top of the digesters, compress and then discharge it through a series of bottom diffusers or radially placed top-mounted lances. In the latter systems, biogas is collected at the top of the anaerobic digesters, compressed, and discharged through confined tubes where an airlift effect is induced. The design of gas mixing systems is currently based on empirical correlations using the power input per unit volume [W/m³], the gas flowrate per unit volume of sludge [m³/(h·m³)], total solids (TS) [%], sludge rheology, and digester aspect ratio. Gas mixing systems have the advantage that they do not need moving parts installed inside the digester ([Lindmark *et al.* 2014](#)).

Pumping systems withdraw a portion of the biomass and reinject it tangentially through nozzles at the bottom of the tank ([Sajjadi *et al.* 2016](#)). This type of mixing, however, has been reported to be the least effective and has been rarely used alone for mixing ([Tang 2009](#)). Pumped recirculation does not increase the mixing, despite it having a strong influence on flow pattern ([Meister *et al.* 2018](#)).

[Vesvikar & Al-Dahhn \(2005\)](#) indicated that areas in which the speed was less than 5% of the maximum speed were considered as dead or inactive zones. Formation of dead zones depends on the viscosity of slurry which increases with the increasing of the TS content, as later shown in the sludge rheology sub-section. To quantify velocity fields, [Wu \(2010\)](#) defined three velocity ranges:

- areas with low velocity ($0 < v < 0.05$ m/s),
- areas with medium velocity ($0.05 < v < 1$ m/s),
- areas with high velocity ($v > 1$ m/s).

The turbulent kinetic energy ([Sindall *et al.* 2013](#)) and the shear rate at the bottom ([Leonzio 2018](#)) represent other parameters to characterize mixing in anaerobic digesters. Other mixing indicators are given in [Teixeira & Do Nascimento Siqueira \(2008\)](#), [Gualtieri \(2010\)](#), [Angeloudis *et al.* \(2016\)](#) and [Ouro *et al.* \(2018\)](#).

Although computational fluid dynamics (CFD) is widely applied to investigate environmental flows ([Blocken & Gualtieri 2012](#); [Amicarelli *et al.* 2020](#)) as it enables the numerical simulation of flow patterns as well as various output parameters in anaerobic digesters, e.g. vorticity, turbulence levels, etc., the number of CFD studies on anaerobic digestion is still limited ([Table 1](#)). The main challenge arises in the attempt of successfully simulating a time varying process, solving the Navier-Stokes equations adapted to account for the presence of a non-Newtonian fluid flow. Investigations of digester mixing using CFD have been performed by many researchers, e.g. [Wu & Chen \(2008\)](#), [Terashima *et al.* \(2009\)](#), [Martínez Mendoza *et al.* \(2011\)](#), [Wu \(2011, 2012, 2014\)](#), [Dapelo *et al.* \(2015\)](#), [López-Jiménez *et al.* \(2015\)](#), [Dapelo & Bridgeman \(2018\)](#), [Leonzio \(2018\)](#), and [Meister *et al.* \(2018\)](#). [Wu & Chen \(2008\)](#) demonstrated that flow patterns for Newtonian and non-Newtonian fluids are completely different. [Terashima *et al.* \(2009\)](#) evaluated the performance of the laminar flow agitation numerically, introducing the uniformity index parameter. [Martínez Mendoza *et al.* \(2011\)](#) modelled the flow inside an anaerobic digester numerically, showing that the distribution of velocities and streamlines is vital for determining the occurrence of dead regions. [Manea & Robescu \(2012\)](#) developed three-dimensional numerical simulations, obtaining the optimum geometry and nominal shaft speed for the digester under study. [Wu \(2011\)](#) applied six turbulence models (see [Table 1](#)) to predict mixing flow pattern in a full-size digester. Later on, [Wu \(2012\)](#) simulated the mixing agitation using the large eddy simulation (LES) turbulence method, assuming the sludge as a pseudo-plastic. In this study, [Wu \(2012\)](#) used the sliding mesh method to characterize the impeller rotation.

Table 1 | Applied CFD methods, turbulence models and main results obtained in the surveyed literature

Reference	CFD method	Turbulence model	Main results
Vesvikar & Al-Dahhn (2005)	Finite difference	$k-\varepsilon$ for liquid phase, zero equation model for gas phase	Dead zones, flow pattern, gas distribution
Wu & Chen (2008)	Finite volume	$k-\varepsilon$ for sludge treated as single equivalent phase	Dead zones, flow pattern
Terashima <i>et al.</i> (2009)	Finite element	No turbulence, homogeneous single-phase treated as laminar	Sludge concentration in full-scale anaerobic digester
Wu (2010)	multiple reference frame (MRF) for propeller	$k-\varepsilon$ for sludge treated as single equivalent phase	Dead zones, mixing energy level (Equation (2))
Wu (2011)	MRF for propeller	$k-\varepsilon$ model, RNG $k-\varepsilon$, realizable $k-\varepsilon$ (Shih <i>et al.</i> 1995), standard $k-\omega$, SST $k-\omega$, Reynolds stress model	Flow pattern, power and flow number (Paul <i>et al.</i> 2004)
Wu (2012)	MRF for propeller	Large eddy simulation or sludge treated as single equivalent phase	Flow pattern, power and flow number (Paul <i>et al.</i> 2004)
Manea & Robescu (2012)	MRF for propeller	No turbulence, homogeneous single-phase treated as laminar	Flow pattern, impeller geometry optimization
Wu (2014)	Eulerian multiphase flow model for gas mixing	SST $k-\omega$ model	Flow pattern, velocity gradient (Equation (1)), breakup number (Coufort <i>et al.</i> 2005)
Dapelo <i>et al.</i> (2015)	Euler-Lagrangian multiphase flow model for gas mixing	Reynolds stress model	Flow pattern, shear rate (Leonzio 2018)
López-Jiménez <i>et al.</i> (2015)	Finite volume method	$k-\varepsilon$ for sludge treated as single equivalent phase	Dead zones, flow pattern, recirculation regions
Chandran <i>et al.</i> (2017)	Eulerian multiphase flow model for gas mixing	No turbulence	Velocity magnitude
Dapelo & Bridgeman (2018)	Euler-Lagrangian multiphase flow model for gas mixing	Reynolds stress model	Apparent viscosity (Equation (4)), flow pattern, shear rate (Leonzio 2018)
Leonzio (2018)	Euler-Euler/Euler-Lagrangian multiphase flow model for gas mixing	$k-\varepsilon$ model	Flow pattern, dead zones, shear rate
Torotwa & Ji (2018)	Euler-Euler multiphase flow model for gas mixing	$k-\varepsilon$ model	Sludge concentration in laboratory-scale anaerobic digester, flow pattern

Three subgrid scale (SGS) models are investigated, namely the Smagorinsky-Lilly model, the wall-adapting local eddy-viscosity model, and the kinetic energy transport (KET) model. Again, Wu (2014) simulated the gas mixture using a Eulerian multiphase flow model. The review paper of Lindmark *et al.* (2014) summarized a number of CFD studies evaluating different mixing methods, their modeling approaches and validation methods. López-Jiménez and co-workers (2015) studied the anaerobic digester applying the Reynolds Averaged Navier-Stokes (RANS) equations closed with the standard $k-\varepsilon$ turbulence model. A single-phase model was applied considering both Newtonian and non-Newtonian rheology for the sludge simulations, allowing the identification of dead zones as well as possible shortcuts.

Leonzio (2018) conducted research on the best mixing systems and geometric configuration for an anaerobic digester with CFD analysis. Meister *et al.* (2018) conducted a CFD analysis based on the finite volume method of the mixing of Newtonian and non-Newtonian sludge in anaerobic digesters to investigate the effects of operational variations on TS concentration. The study revealed that the operation with pumped recirculation and impeller rotating within a mechanical draft tube yielded the highest level of mixing. Dapelo & Bridgeman (2018) developed a hybrid Euler-Lagrange (EL) CFD model to simulate an anaerobic digester mixed with gas under pressure. The movement of the sludge is driven by the transfer of the moment from the bubbles to the fluid. Recent comprehensive reviews on CFD applied to anaerobic

digesters can be found in *Sadino-Riquelme et al. (2018)*, *Wang et al. (2018)* and *Singh et al. (2019)*. Table 1 summarizes applied CFD numerical methods for discretizing governing equations, turbulence models and main outcomes for the above discussed reports.

Few reports dealing with the analysis of full-scale anaerobic digesters are available (*Monteith & Stephenson 1981*; *Kushkevych et al. 2020*) because laboratory-scale digesters are typically adopted to evaluate a full-scale application of anaerobic digestion, see e.g. *Wu & Chen (2008)* and *Bouallagui et al. (2010)*. However, scale effects could prevent a straightforward projection of operational data from laboratory-scale results to the full-scale designs.

In this study, full-scale gas mixing and mechanical mixing of a pseudo-plastic sludge of given rheology was compared at same operational conditions: input/treated sludge ($75 \text{ m}^3/\text{day}$), TS (6%), temperature T (35°C) and daily energy consumption E (140.4 kWh). For this purpose, a CFD analysis was carried out, an approach where literature studies are still limited. The comparative analysis was carried out in terms of the distribution of velocity magnitude and pattern, turbulent kinetic energy and the formation of dead zones. Consumed energy E , derived from the real case consisting of a gas mixing anaerobic digester, was kept constant for two hypothetical cases consisting of two mechanical mixings, as next described.

MATERIALS AND METHODS

Case study description

The present fluid-dynamic investigation is referred to one of the two gas mixed anaerobic digesters of the wastewater treatment plant (WWTP) connected to the municipality of

Keszthely (Hungary). The WWTP is designed to serve 125,000 population equivalent (PE) as maximum during the tourist season (*Figure 1(a)*). Each digester is 11.30 m of inner diameter and 16 m high (14 m normal sludge filling level), for a sludge volume $\Omega = 1,404 \text{ m}^3$ per digester.

The sludge quantity and composition are given in *Table 2*.

In the actual configuration, eight vertical lances, 0.075 m of inner diameter and evenly spaced on a 4 m radius ring tube fed by a compressor, inject the biogas at a distance of 0.37 m from the bottom (*Figure 1(b)*). The gas mixing works discontinuously, according to the sequence of 120 min divided into six phases of 20 min each; see *Table 3*. During each phase, a group of four adjacent lances is activated and fed with the full biogas flow delivered by the compressor.

According to the operating conditions adopted for the digesters of the WWTP, the number of working hours in a day of the gas mixing system – considering one single digester – is therefore $n_h = 8$ overall. This modality was recently proved in *Singh et al. (2019, 2020)* as the best to maximize biogas production in intermittent mixing. The electric power absorbed by the compressor is calculated by means of the following equation:

$$P = \frac{Q_g dp p_s}{1000} [\text{kW}] \quad (1)$$

where $Q_g = 282 \text{ Nm}^3/\text{h}$ is the total biogas flow rate at normal conditions delivered by the compressor, $dp = 147.1 \text{ kPa}$ is the compressor discharge pressure, $p_s = 0.423 \text{ Wh}/(\text{Nm}^3 \text{ kPa})$ is the compressor specific power consumption (*Table 4*). Daily averaged energy consumption for one digester is therefore given by $E = P n_h = 140.4 \text{ kWh}$.

In the present study, we consider two long shafted paddle mixing impellers as possible alternatives to the

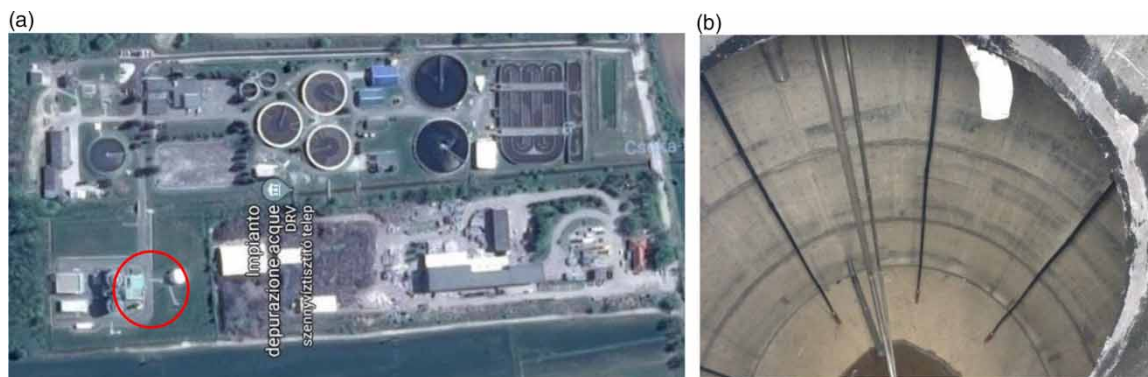


Figure 1 | (a) WWTP in Keszthely (Hungary). Red circle indicates the position of the digesters. (b) Inner side of one of the digesters with the gas recirculation lances. Please refer to the online version of this paper to see this figure in colour: <http://dx.doi.org/10.2166/wst.2020.248>.

Table 2 | Sludge quantity and composition (total for both digesters)

	Primary sludge	Biologic excess sludge
Volumetric flow [m ³ /d]	83	68
Dry solids (DS) concentration [kg/m ³]	61	61
Organic dry solids (ODS) [%]	71	61

gas mixing system. The geometric specifications of the digester's shape and adopted mixers are summarized in Table 4.

The rpm of the mixer blades is derived on the basis of the P-rpm relationship given in Table S1, Supplementary material.

The linear regression yields for Mixer 1:

$$P_1 = 0.2109\text{rpm} - 0.4014 \quad R^2 = 0.9984 \quad (2)$$

whereas Mixer 2 is well described by a linear function crossing the origin (0,0):

$$P_2 = 0.27 \text{ rpm} \quad (3)$$

Power consumption for mechanical mixing (working continuously 24 h) was derived by keeping E constant. Since the daily averaged power consumption for one digester is $\bar{P} = E/24 = 5.87 \text{ kW}$, the number of revolutions therefore adopted are $\text{rpm}_1 = 29.9 \text{ min}^{-1}$ (from Equation (2)) and $\text{rpm}_2 = 21.6 \text{ min}^{-1}$ (from Equation (3)) for Mixer 1 and Mixer 2 respectively.

Sludge rheology

Sludge in anaerobic digesters as wastewater, slurries from food processing plants and animal manure exhibit a non-Newtonian behaviour (Sajjadi *et al.* 2016). In particular, slurry flows with TS $\geq 2.5\%$ can be described as non-Newtonian pseudo-plastic fluids (Meister *et al.* 2018). From a general point of view, the stress tensor τ [Pa] is defined in terms of the shear rate tensor γ' [s⁻¹] and the dynamic viscosity η [Pa s]:

$$\tau_{ij} = \eta \gamma'_{ij} \quad (4)$$

in which the shear rate components are given by

$$\gamma'_{ij} = (\partial u_i / \partial x_j + \partial u_j / \partial x_i) \quad (5)$$

Table 3 | Sequence of lances operations for the biogas mixing on the digesters, referred to as 'A' and 'B', respectively, of the Keszthely WWTP

Phase nr.	1	2	3	4	5	6
Phase duration [min]	20	20	20	20	20	20
Cumulative time [min]	20	40	60	80	100	120
Action	digester A, lances 1 – 4	pause	digester B, lances 1 – 4	digester A, lances 5 – 8	pause	digester B, lances 5 – 8

Table 4 | Digester's geometry and adopted mixers

Digester inner diameter [m]	Digester total height [m]	Sludge filling level in digester [m]	Total sludge volume [m ³]	Daily treated sludge volume [m ³ /d]
11.30	16	14	1,404	75
Gas mixing	Lances' outlet from bottom [m]	Discharge pressure [kPa]	Total gas volume flow rate [Nm³/h]	Specific power [Wh/(Nm³ kPa)]
8 lances $\phi 75$ mm half working at a time	0.37	147.1	282	0.423
Mixer 1	Diameter [m]	Distance from the bottom [m]	Distance between impellers [m]	
Propeller, 2 impellers, 2 blades per impeller	2.5	3.0	8.8	
Mixer 2	Diameter [m]	Distance to the bottom [m]	Distance between impellers (not equally spaced) [m]	
Propeller, 3 impellers, 2 blades per impeller	3.1	3.0	Upper spacing: 2.3 Lower spacing: 6.6	

where u_i is the scalar component of velocity field \vec{v} , along the x_i coordinate axis.

In this study, the viscosity appearing in Equation (4) is modelled as a function of the shear rate magnitude $|\dot{\gamma}'|$ using a power-law relationship (Rendina *et al.* 2019):

$$\eta = K|\dot{\gamma}'|^{n-1} \quad (6)$$

where K [Pa·sⁿ] is the consistency coefficient and n is the power-law index. The equation holds for the interval $\zeta = (|\dot{\gamma}'|_{\min}; |\dot{\gamma}'|_{\max})$ depending on the content of TS (Wu & Chen 2008; Bridgeman 2012); see Table S2, Supplementary material. Beyond ζ limits, viscosity takes constant minimum η_{\min} and maximum η_{\max} values to prevent singularities when computing runs take place. Rheology parameters strongly depend on TS (Wu & Chen 2008) and temperature T as depicted in Table S2 (Achhari-Begdouri & Goodrich 1992).

From Table S2, the following regressions, either linear or exponential, are derived:

$$K = 0.0117 e^{0.5078TS} \quad R^2 = 0.9983 \quad (7)$$

$$n = -0.034 TS + 0.7793 \quad R^2 = 0.9777 \quad (8)$$

$$\rho = 0.1425 TS + 999.99 \quad R^2 = 0.9956 \quad (9)$$

Parameters' values were derived from regressions, Equations (7)–(9), assuming the sludge isothermal and incompressible; see Table 5.

Numerical setup

The Level Set Two-Phase Flow method (Olsson & Kreiss 2005; Bovolin *et al.* 2017) is adopted to model fluid–gas interaction in the case of gas mixing. The Level Set method allows to simulate two immiscible fluids separated by moving interfaces making use of a level set function, that is a smooth continuous function $\varphi[\vec{x}(t)] \in [0, 1]$ whose value defines the phase locally:

$$\varphi \begin{cases} > 0.5 & \text{fluid} \\ = 0.5 & \text{interface} \\ < 0.5 & \text{air} \end{cases} \quad (10)$$

Table 5 | Derived parameters' values for the sludge at $T = 35^\circ\text{C}$ with $TS = 6\%$

TS [%]	K [Pa s ⁿ]	n [-]	ρ [kg/m ³]
6	0.246	0.575	1,000.85

The evolution of φ is described by the following transport equation:

$$\vec{v} \cdot \vec{\nabla} \varphi = \gamma \vec{\nabla} \cdot (\varepsilon \vec{\nabla} \varphi - \varphi(1 - \varphi) \vec{n}) \quad (11)$$

where ε and γ are the stabilization and reinitialization terms respectively, $\vec{n} = \frac{\vec{\nabla} \varphi}{|\vec{\nabla} \varphi|}$ is the unit normal vector. Sludge motion is modelled as incompressible, spatially integrating over a finite element grid the unsteady Reynolds-averaged Navier–Stokes (RANS) equations, modified for non-Newtonian rheology:

$$\vec{\nabla} \cdot \vec{v} = \vec{0} \quad (12)$$

$$\rho \left(\frac{\partial}{\partial t} + \vec{v} \cdot \vec{\nabla} \right) \vec{v} = -\vec{\nabla} p + \vec{\nabla} \cdot \tau + \rho \vec{g} + \sigma \kappa \vec{n} \quad (13)$$

where the τ_{ij} components are given by Equation (4), $\vec{\nabla}$ is the symbolic operator of components $(\partial/\partial x, \partial/\partial y, \partial/\partial z)$, \vec{v} is the velocity field, \vec{g} is the gravity acceleration, p is the pressure, ' \cdot ' is the symbol of the scalar product:

$$\rho = \rho_a + (\rho_f - \rho_a) \varphi \quad (14)$$

$$\eta = \eta_f + (\eta_f - \eta_a) \varphi \quad (15)$$

are the local density and the dynamic viscosity obtained by linearly averaging between corresponding values for the fluid (f) and air (a). Last term on the right hand side of Equation (13) represents the surface specific tension force which arises over interfaces: $\sigma = 0.0705$ N/m is the tension coefficient, here assumed as for water–air, δ is the Dirac delta function and $\kappa = \vec{\nabla} \cdot \vec{n}$ is the local interface curvature field. Turbulence is modelled using the standard two-equation k - ε model (Launder & Spalding 1974), based on the transport equations for kinetic turbulent energy (k) and the dissipation rate (ε). The k - ε model has been successfully used by many researchers for related mixing problems in anaerobic digesters (Meroney & Colorado 2009; López-Jiménez *et al.* 2015).

Gas inlet is set at the lower end of four adjacent lances, each lance issuing a gas flow rate of 10.2 L/s. Gas outlet is set at the upper free surface of the sludge. Simulation domain corresponds to the inner space of digester with the presence of the eight lances, see Figure 2(a).

In the case of mechanical mixing (Figure 2(b) and 2(c)), the rotating domain is modelled using a homogeneous single-phase turbulent non-Newtonian flow. The steady Navier–Stokes equations formulated in the rotating

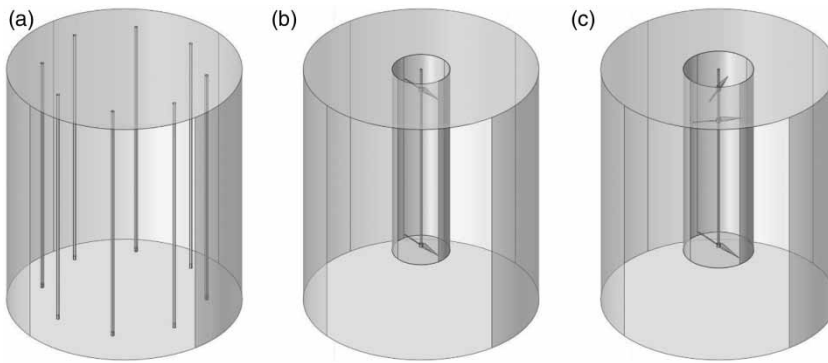


Figure 2 | Computational domain. (a) Gas mixing. (b) Mixer 1. (c) Mixer 2.

coordinate system:

$$\vec{\nabla} \cdot \vec{v} = \vec{0} \quad (16)$$

$$\rho \vec{\omega} \vec{\nabla} \vec{\omega} + 2\rho \vec{\Omega} \times \vec{\omega} = -\vec{\nabla} p + \vec{\nabla} \cdot \tau + \rho \left[\vec{g} - \frac{\partial \vec{\Omega}}{\partial t} \times \vec{r} + \vec{\Omega} \times (\vec{\Omega} \times \vec{r}) \right] \quad (17)$$

are solved with reference to the velocity vector $\vec{\omega}$, referred to the rotating coordinate system. In the above Equations (16) and (17), \vec{r} is the position vector while $\vec{\Omega}$ is the angular velocity vector. In the global coordinate system, the velocity vector \vec{v} is related to the moving component $\vec{\omega}$ by means of:

$$\vec{v} = \vec{\omega} + \frac{\partial \vec{r}}{\partial t} \quad (18)$$

Mesh generation

In the case of gas mixing, the lances are treated as void spaces. The mesh is finer where gas inlet is set, since the inlet gas flow velocity is the highest in this region. In the case of mechanical mixing, two regions with different mesh quality are introduced. The mesh of the rotating domain is finer than the mesh of the rest of the domain since the flow velocity is higher in this region.

The spatial decomposition is made by using unstructured meshes of tetrahedral elements. Finer boundary layer mesh elements are set at the walls to comply with the constraints imposed by the adopted k- ϵ turbulence model. Sharp corners are avoided because they may introduce singularities in the solution.

Mesh convergence study

Three levels of spatial discretization are tested, respectively indicated as meshes 1, 2 and 3 in Table 6 (gas mixing) and

Table 6 | Mesh properties in the case of gas mixing

Mesh parameters	Mesh 1	Mesh 2	Mesh 3
Max cell size [m]	1.980	1.650	1.254
Min cell size [m]	0.099	0.099	0.0099
Number of cells	36,323	62,566	123,931

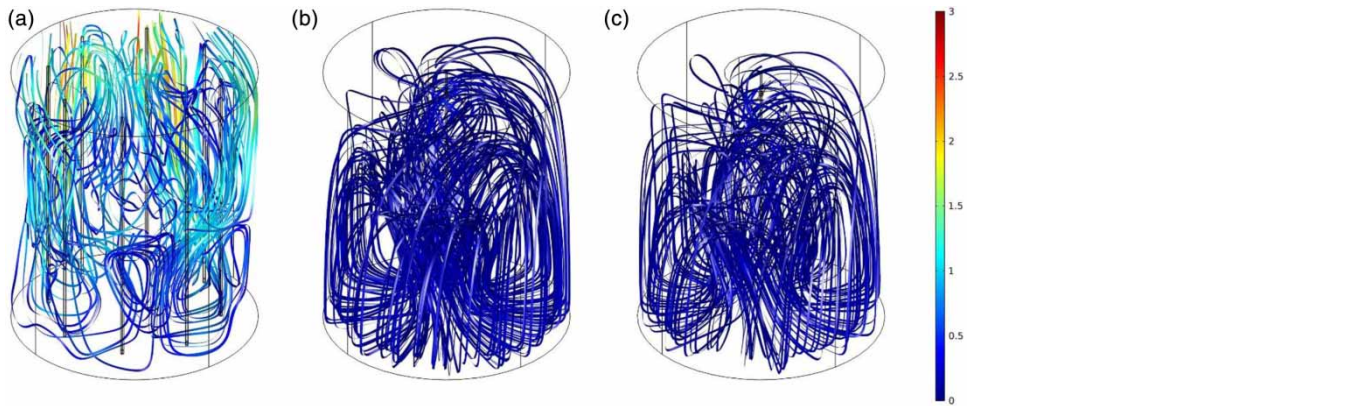
Table 7 (Mixer 1). The successive refined meshes yielded convergent solutions starting from mesh 2 for all cases, thus making the FSI computations reliable. Results next presented are obtained with such level of discretization.

RESULTS AND DISCUSSION

The evaluation of the mixing is done by computing the velocity magnitude and pattern, the turbulent kinetic energy and the formation of dead zones. Results are presented when nearly steady state conditions are reached as in *Viccone et al. (2012)* in the case of gas mixing. Dead zones refer to the regions of the digester where the velocity is smaller than 0.05 m/s according to *Wu (2010)*. Computed quantities are all referred to the inner volume Ω of the digester. The analysis of the velocity pattern shows that a convective movement of the sludge is created inside the digester; see *Figure 3*. In the central section of the digester a large downward flow is created in the central part with vortices located near the bottom of the digester. In the case of gas mixing (*Figure 3(a)*), higher velocity magnitudes are attained of the order of 1 m/s near the walls. This is basically due to the thrust exerted by air bubbles on the sludge when moving upwards to the free surface. In the case of mechanical mixing (*Figure 3(b)* and *3(c)*), the velocity magnitudes were generally dramatically lower, with peaks of

Table 7 | Mesh properties in the case of Mixer 1

Mesh parameters	Mesh 1		Mesh 2		Mesh 3	
	Rotating domain	Outer domain	Rotating domain	Outer domain	Rotating domain	Outer domain
Max cell size [m]	0.0053	0.013	0.004	0.01	0.003	0.007
Min cell size [m]	0.01	0.006	0.001	0.005	0.001	0.004
Number of cells	26,696	204,432	41,094	334,752	66,766	672,912

**Figure 3** | 3D trajectory extraction. Colour is related to the velocity magnitude [m/s]. (a) Gas mixing. (b) Mixer 1. (c) Mixer 2. Please refer to the online version of this paper to see this figure in colour: <http://dx.doi.org/10.2166/wst.2020.248>.

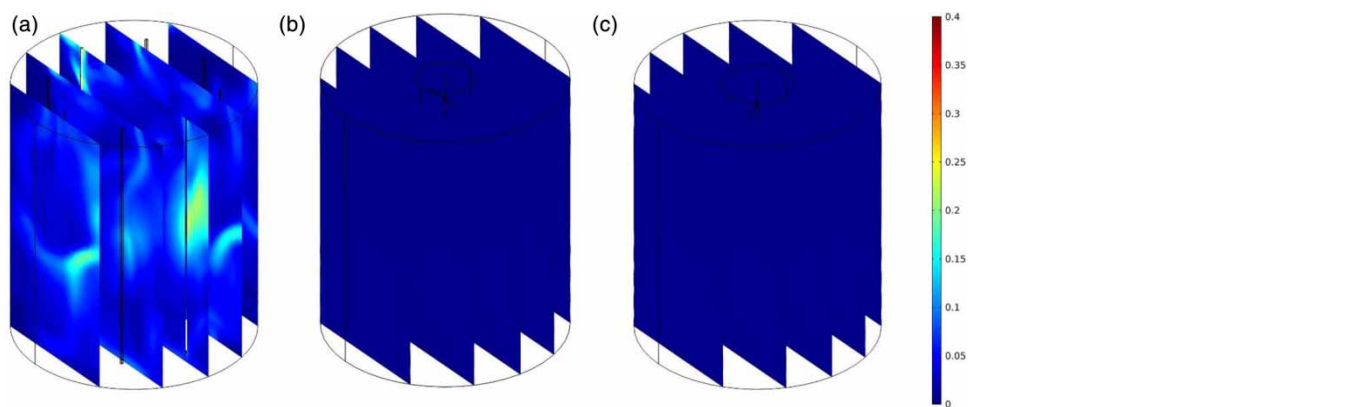
1.33 m/s nearby the paddle blades for Mixer 1 (see Figure S1, Supplementary material).

The results concerning the turbulent kinetic energy [m^2/s^2] reveal a level of agitation at the upper part of the digester with a maximum value of $0.24 \text{ m}^2/\text{s}^2$ in the case of gas mixing (Figure 4(a)). This is an expected result as the gas bubbles finally break at the free surface, generating turbulence nearby. From an operational point of view, this aspect is very useful because it helps the digester function against the formation of crusts. In the case of mechanical

mixing, turbulence levels are negligible as can be seen in Figure 4(b) and 4(c).

As concerning the formation of dead zones, half of the digester inner volume Ω participates actively in the mixing process, in the case of mechanical mixing (Figure 5(b) and 5(c)). Most of the stagnant regions are located near the vertical wall and at the free surface, whereas the inner regions near the paddle blades feature high levels of velocity.

In the case of gas mixing, dead zones are present far away from the gas inlet areas as depicted in Figure 5(a),

**Figure 4** | Turbulent kinetic energy [m^2/s^2]. (a) Gas mixing. (b) Mixer 1. (c) Mixer 2.

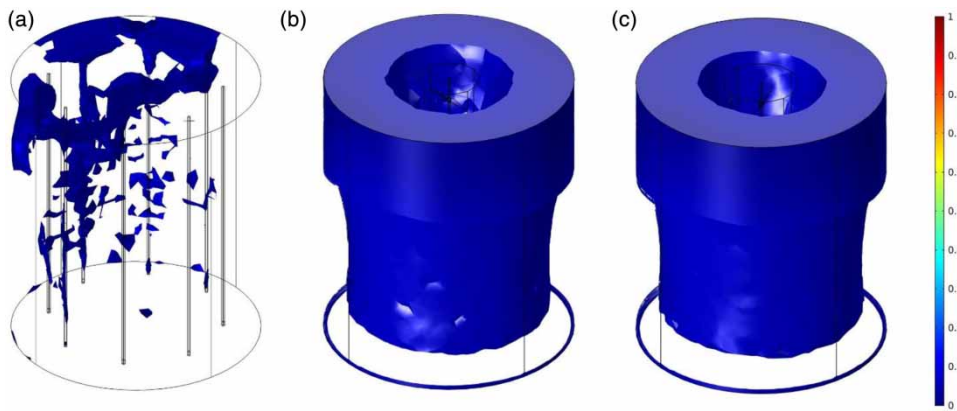


Figure 5 | Dead zones, defined on the basis of the condition $v < 0.05$ m/s. Colour contour is set with the upper value (unity) related to the threshold velocity. (a) Gas mixing. (b) Mixer 1. (c) Mixer 2. Please refer to the online version of this paper to see this figure in colour: <http://dx.doi.org/10.2166/wst.2020.248>.

attaining the mean value of about 4.8% (bold value in Table 8). Geometry optimization concerning the digester shape, length, distance to the bottom and diameter of lances would certainly allow a further decrease (Singh *et al.* 2019). In the following Table 8, a summary of the obtained numerical results is presented. The ‘intermediate velocity zones’ refers to the volume (in percentage in respect of the inner volume) where velocity ranges in the interval $0.05 < v < 1$ m/s, whereas the ‘high velocity zones’ refers to velocities higher than 1 m/s.

The best solution, considering the same daily energy consumption E , is given by the gas mixing solution. In fact, in Table 8 it is shown that dead regions are about a tenth of mechanical mixing (4.8% vs 50.6% for Mixer 1 and 51.3% for Mixer 2) while spatially averaged velocity is about four times greater (0.31 m/s vs 0.07 m/s for Mixer 1 and Mixer 2). This is basically due to the corresponding low number of revolutions for the adopted Mixers ($\text{rpm}_1 = 29.9 \text{ min}^{-1}$ and $\text{rpm}_2 = 21.6 \text{ min}^{-1}$, respectively). In López-Jiménez *et al.* (2015) the simulation of flow patterns was carried out using a propeller rotating from 400 to 750 rpm,

which is one order of magnitude greater. Dead zones, however defined on the less restrictive criterion $v < 0.05$ m/s were 0.21% and 4.2% for non-Newtonian sludge with $\text{TS} = 2.5\%$ and 5.4% respectively. Manea & Robescu (2012) recommended axial mixers having four to six blades, with a tilt angle between 15° and 45° and shaft speeds between 100 and 800 rpm. In addition, six new simulations (three per mixer) were carried out with the parameters listed in Table 5, to compare the effect of increased mixing speeds of 50, 100 and 200 rpm on the percentage of dead zones (DVP), without caring of the mixer rpm operational range (see specifications in Table S1). Once again, dead volumes were assessed on the basis of the condition $v < 0.05$ m/s. Results are summarized in Table 9.

Daily energy consumptions E are derived from Equations (2) and (3), for Mixers 1 and 2, respectively, under the same condition of mixing operating 24 h per day. As can be noted, the increase of rpm corresponds to a fast decrease of DVP but at the expense of higher E levels. Above $\text{rpm} = 100$, stagnant regions occupy less than 1% of the digester’s volume, at the cost of tripled energy

Table 8 | Main numerical results

Parameter	Gas mixing			
	Mean value	Standard deviation	Mixer 1	Mixer 2
Max velocity [m/s]	3.03	0.20	1.33	1.00
Spatially averaged velocity [m/s]	0.31	0.09	0.07	0.07
Spatially averaged turbulent kinetic energy [m^2/s^2]	0.23	0.10	0.001	0.001
Dead zones [m^3]	63.64 (4.8%)	42.08 (3.2%)	665.83 (50.6%)	674.91 (51.3%)
Intermediate velocity zones [m^3]	1,237.64 (94.1%)	26.89 (2.0%)	649.12 (49.4%)	639.87 (48.7%)
High velocity zones [m^3]	13.68 (1.0%)	19.74 (1.5%)	0.00 (0.0%)	0.00 (0.0%)

Table 9 | Impact of mixing speed (rpm) on dead volume percentages (DVP) and consumed energy (E) for Mixer 1 and Mixer 2

Mixer 1			Mixer 2		
rpm [min ⁻¹]	DVP [%]	E [kWh]	rpm [min ⁻¹]	DVP [%]	E [kWh]
29.9	50.6	140	21.6	51.3	140
50	21.6	243	50	2.9	324
100	0.4	496	100	0.1	648
150	0.1	750	150	0.0	972

values or more, compared with the reference value $E = 140.4$ kWh. Geometry optimization of the mechanical mixing systems can lead to a drastic reduction of dead zones (Singh et al. 2019) as well. This implies a sensitivity analysis based on the geometry of the mixer (number of impellers, number of blades per impeller, the blade's profile) which is out of the scope of this paper.

In terms of turbulent agitation, mechanical mixing does not exhibit significant levels, proving that this technology is appropriate only for convective movement.

CONCLUSIONS

Anaerobic digestion is largely applied for the stabilization of sewage sludge and landfill leachate. The production of biogas is beneficial for the environment, helping the reduction of greenhouse emissions. The efficiency of digestion process is affected by several operating parameters including the rate of mixing, which was commonly studied in the past at a laboratory scale.

In this study, a three-dimensional CFD steady/unsteady model was developed and applied to quantify mixing in a full-scale anaerobic digester. Non-Newtonian properties of the sludge, consisting of a pseudo-plastic fluid, were taken into account in the closure of governing equations. Stirred and gas mixing solutions were compared in terms of flow patterns, turbulent kinetic energy and dead zones, keeping fixed the daily energy consumption. In the case of gas mixing, the real configuration of the lances and their operating conditions were adopted. For the mechanical mixing, two central draft tube mixers with two (Mixer 1) and three (Mixer 2) impellers, respectively, were comparatively studied. The number of rounds per minute were derived from the given P-rpm curves, under continuous mixing. Gas mixing was found to be preferable to mechanical mixing in terms of mixing performances, namely:

- maximum velocity was about three times larger than that associated with mechanical mixing systems;
- dead zones percentage was one order of magnitude lower (about 5% against 50%);
- turbulent kinetic energy was two orders of magnitude larger ($0.24 \text{ m}^2/\text{s}^2$ against $0.001 \text{ m}^2/\text{s}^2$). Maximum values were attained over the upper part of the digester, with a positive effect against the formation of crusts.

Increasing impeller speed helps reduce stagnant regions but at the cost of higher electric energy consumption.

SUPPLEMENTARY MATERIAL

The Supplementary Material for this paper is available online at <https://dx.doi.org/10.2166/wst.2020.248>.

REFERENCES

- Abuabdou, S. M. A., Bashir, M. J. K., Aun, N. C. & Sethupathi, S. 2018 *Applicability of anaerobic membrane bioreactors for landfill leachate treatment: review and opportunity*. *IOP Conference Series: Earth and Environmental Science* **140** (1), 012033. doi: 10.1088/1755-1315/140/1/012033.
- Abuabdou, S. M. A., Ahmad, W., Aun, N. C. & Bashir, M. J. K. 2020 *A review of anaerobic membrane bioreactors (AnMBR) for the treatment of highly contaminated landfill leachate and biogas production: effectiveness, limitations and future perspectives*. *Journal of Cleaner Production* **255**, 120215. doi: 10.1016/j.jclepro.2020.120215.
- Achkari-Begdouri, A. & Goodrich, P. R. 1992 *Rheological properties of Moroccan dairy cattle manure*. *Bioresource Technology* **40**, 149–156. doi: 10.1016/0960-8524(92)90201-8.
- Amicarelli, A., Manenti, S., Albano, R., Agate, G., Paggi, M., Longoni, L., Mirauda, D., Ziane, L., Viccione, G., Todeschini, S., Sole, A., Baldini, L. M., Brambilla, D., Papini, M., Khellaf, M. C., Tagliaferro, B., Sarno, L. & Pirovano, G. 2020 *SPHERA v.9.0.0: a computational fluid dynamics research code, based on the smoothed particle hydrodynamics meshless method*. *Computer Physics Communications* **250**, 107157. doi: 10.1016/j.cpc.2020.107157.
- Angelidaki, I., Ellegaard, L. & Ahring, B. K. 2003 *Applications of the anaerobic digestion process*. *Advances in Biochemistry/Engineering Biotechnology* **82**, 1–33. doi: 10.1007/3-540-45838-7_1.
- Angeloudis, A., Stoesser, T., Gualtieri, C. & Falconer, R. A. 2016 *Contact tank design effect on process performance*. *Environmental Modeling & Assessment* **21** (5), 563–576. doi: 10.1007/s10666-016-9502-x.
- Appels, L., Baeyens, J., Degève, J. & Dewil, R. 2008 *Principles and potential of anaerobic digestion of waste-activated sludge*. *Progress in Energy and Combustion Science* **34** (6), 755–781. doi: 10.1016/j.peccs.2008.06.002.

- Blocken, B. & Gualtieri, C. 2012 Ten iterative steps for model development and evaluation applied to computational fluid dynamics for environmental fluid mechanics. *Environmental Modelling & Software* **33** (7), 1–22. doi:10.1016/j.envsoft.2012.02.001.
- Borole, A. P., Klasson, K. T., Ridenour, W., Holland, J., Karim, K. & Al-Dahhan, M. H. 2006 Methane production in a 100-L upflow bioreactor by anaerobic digestion of farm waste. *Applied Biochemistry and Biotechnology* **131** (1–3), 887–896. doi:10.1385/ABAB:131:1:887.
- Bouallagui, H., Marouani, L. & Hamdi, M. 2010 Performances comparison between laboratory and full-scale anaerobic digesters treating a mixture of primary and waste activated sludge. *Resources, Conservation and Recycling* **55** (1), 29–33. doi: 10.1016/j.resconrec.2010.06.012.
- Bovolin, V., Viccione, G., Di Leo, A. & Dentale, F. 2017 A comparative numerical study of the coanda effect. In: *AIMETA 2017 - Proceedings of the 23rd Conference of the Italian Association of Theoretical and Applied Mechanics*, Vol. 2, pp. 1743–1753.
- Bridgeman, J. 2012 Computational fluid dynamics modelling of sewage sludge mixing in an anaerobic digester. *Advances in Engineering Software* **44**, 54–62. doi: 10.1016/j.advengsoft.2011.05.037.
- Chandran, J., Yogaraj, D., Manikandan, K. & Jeyaraman, P. 2017 Optimization of bio gas recirculation velocity in biogas mixing anaerobic digester with the feed of 8% TDS using CFD. *International Journal of Mechanical Engineering and Technology* **8** (8), 596–606.
- Coufort, C., Bouyer, D. & Line, A. 2005 Flocculation related to local hydrodynamics in a Taylor-Couette reactor and in a Jar. *Chemical Engineering Science* **60**, 2179–2192. doi: 10.1016/j.ces.2004.10.038.
- Dapelo, D. 2016 *Gas Mixing in Anaerobic Digestion*. Ph.D. Thesis, University of Birmingham, Birmingham, UK.
- Dapelo, D. & Bridgeman, J. 2018 Euler-lagrange computational fluid dynamics simulation of a full-scale unconfined anaerobic digester for wastewater sludge treatment. *Advances in Engineering Software* **117**, 153–169. doi: 10.1016/j.advengsoft.2017.08.009.
- Dapelo, D., Alberini, F. & Bridgeman, J. 2015 Euler-Lagrange CFD modelling of unconfined gas mixing in anaerobic digestion. *Water Research* **85**, 497–511. doi: 10.1016/j.watres.2015.08.042.
- DWA-Themenband 2015 Schlammfäulung oder gemeinsame aerobe Stabilisierung bei Kläranlagen kleiner und mittlerer Größe, T1/2015, Deutsche Vereinigung für Wasserwirtschaft, Abwasser und Abfall e.V., Henschel, Germany.
- Ghaly, A. 1989 Continuous production of biogas from dairy manure using an innovative no-mix reactor. *Applied Biochemistry and Biotechnology* **20–21** (1), 541–559. doi: 10.1007/BF02936508.
- Gualtieri, C. 2010 Discussion on E.C.Teixeira and R.N.Siqueira: performance assessment of hydraulic efficiency indexes. *Journal of Environmental Engineering* **136** (9), 1006–1007. ASCE. doi: 10.1061/(ASCE)EE.1943-7870.0000088.
- Kariyama, I. D., Zhai, X. & Wu, B. 2018 Influence of mixing on anaerobic digestion efficiency in stirred tank digesters: a review. *Water Research* **143**, 503–517. doi: 10.1016/j.watres.2018.06.065.
- Kushkevych, I., Cejnar, J., Vítězová, M., Vítěz, T., Dordević, D. & Bomble, Y. 2020 Occurrence of thermophilic microorganisms in different full scale biogas plants. *International Journal of Molecular Science* **21** (1), 283. doi: 10.3390/ijms21010283.
- Lauder, B. E. & Spalding, D. B. 1974 The numerical computation of turbulent flows. *Computer Methods in Applied Mechanics and Engineering* **3** (2), 269–289. doi: 10.1016/0045-7825(74)90029-2.
- Leite, W., Magnus, B. S., Guimarães, L. B., Gottardo, M. & Belli Filho, P. 2017 Feasibility of thermophilic anaerobic processes for treating waste activated sludge under low HRT and intermittent mixing. *Journal of Environmental Management* **201**, 335–344. doi: 10.1016/j.jenvman.2017.06.069.
- Leonzio, G. 2018 Study of mixing system and geometric configurations for anaerobic digesters using CFD analysis. *Renewable Energy* **123**, 578–589. doi: 10.1016/j.renene.2018.02.071.
- Lin, H., Peng, W., Zhang, M., Chen, J., Hong, H. & Zhang, Y. 2013 A review on anaerobic membrane bioreactors: applications, membrane fouling and future perspectives. *Desalination* **314**, 169–188. doi: 10.1016/j.desal.2013.01.019.
- Lindmark, J., Thorin, E., Bel Fdhila, R. & Dahlquist, E. 2014 The effects of different mixing intensities during anaerobic digestion of the organic fraction of municipal solid waste. *Waste Management* **34** (8), 1391–1397. doi: 10.1016/j.wasman.2014.04.006.
- Lisowij, M. & Wright, M. M. 2020 A review of biogas and an assessment of its economic impact and future role as a renewable energy source. *Reviews in Chemical Engineering* **36** (3), 401–421. doi: 10.1515/revce-2017-0103.
- López-Jiménez, P. A., Escudero-González, J., Montoya Martínez, T., Fajardo Montañana, V. & Gualtieri, C. 2015 Application of CFD methods to an anaerobic digester: the case of Ontinyent WWTP, Valencia, Spain. *Journal of Water Process Engineering* **7**, 131–140. doi: 10.1016/j.jwpe.2015.05.006.
- Manea, E. & Robescu, D. 2012 Simulation of mechanical mixing in anaerobic digesters. *UPB Scientific Bulletin, Series D* **74** (2), 235–242.
- Martínez Mendoza, A., Montoya Martínez, T., Fajardo Montañana, V. & López Jiménez, P. A. 2011 Modeling flow inside an anaerobic digester by CFD techniques. *International Journal of Energy and Environment* **2** (6), 963–974.
- Meegoda, J. N., Li, B., Patel, K. & Wang, L. B. 2018 A review of the processes, parameters, and optimization of anaerobic digestion. *International Journal of Environmental Research and Public Health* **15** (10), 2224. doi: 10.3390/ijerph15102224.
- Meister, M., Rezavand, M., Ebner, C., Pumpel, T. & Rauch, W. 2018 Mixing non-Newtonian flows in anaerobic digesters by impellers and pumped recirculation. *Advances in Engineering Software* **115**, 194–203. doi: 10.1016/j.advengsoft.2017.09.015.

- Meroney, R. N. & Colorado, P. E. 2009 CFD simulation of mechanical draft tube mixing in anaerobic digester tanks. *Water Research* **43**, 1040–1050. doi: 10.1016/j.watres.2008.11.035.
- Monteith, H. D. & Stephenson, J. P. 1981 Mixing efficiencies in full-scale anaerobic digesters by tracer methods. *Journal of the Water Pollution Control Federation* **53** (1), 78–84.
- MULEWF 2014 *Umstellung von Kläranlagen auf Schlamm Faulung*. Report, Ministerium für Umwelt, Landwirtschaft, Ernährung, Weinbau und Forsten Rheinland-Pfalz, Germany. https://mueef.rlp.de/fileadmin/mulewf/Publikationen/Umstellung_von_Klaeranlagen_auf_Schlammfaulung.pdf (accessed 22 February 2020)
- Olsson, E. & Kreiss, G. 2005 A conservative level set method for two phase flow. *Journal of Computational Physics* **210**, 225–246. doi: 10.1016/j.jcp.2005.04.007.
- Ouro, P., Fraga, B., Viti, N., Angeloudis, A., Stoesser, T. & Gualtieri, C. 2018 Instantaneous transport of a passive scalar in a turbulent separated flow. *Environmental Fluid Mechanics* **18** (2), 487–513. doi: 10.1007/s10652-017-9567-3.
- Paul, E. L., Atiemo-Obeng, V. A. & Kresta, S. M. 2004 *Handbook of Industrial Mixing: Science and Practice*. Wiley and Sons Inc, Hoboken, NJ, USA.
- Qasim, S. R. 1999 *Wastewater Treatment Plants: Planning, Design and Operation*. CRC Press, Boca Raton, FL, USA.
- Rendina, I., Viccione, G. & Cascini, L. 2019 Kinematics of flow mass movements on inclined surfaces. *Theoretical and Computational Fluid Dynamics* **33** (2), 107–123. doi: 10.1007/s00162-019-00486-y.
- Sadino-Riquelme, C., Hayes, R. E., Jeison, D. & Donoso-Bravo, A. 2018 Computational fluid dynamic (CFD) modelling in anaerobic digestion: general application and recent advances. *Critical Reviews in Environmental Science and Technology* **48** (1), 39–76. doi: 10.1080/10643389.2018.1440853.
- Sajjadi, B., Raman, A. A. A. & Parthasarathy, R. 2016 Fluid dynamic analysis of non-Newtonian flow behavior of municipal sludge simulant in anaerobic digesters using submerged, recirculating jets. *Chemical Engineering Journal* **298**, 259–270. doi: 10.1016/j.cej.2016.03.069.
- Serna-Maza, A., Heaven, S. & Banks, C. J. 2017 *In situ* biogas stripping of ammonia from a digester using a gas mixing system. *Environmental Technology* **38** (24), 3216–3224. doi: 10.1080/09593330.2017.1291761.
- Shi, X.-S., Dong, J.-J., Yu, J.-H., Yin, H., Hu, S.-M., Huang, S.-X. & Yuan, X.-Z. 2017 Effect of hydraulic retention time on anaerobic digestion of wheat straw in the semicontinuous continuous stirred-tank reactors. *BioMed Research International* **2457805**. doi: 10.1155/2017/2457805.
- Shih, T.-H., Liou, W. W., Shabbir, A., Yang, Z. & Zhu, J. 1995 A new $k-\epsilon$ eddy viscosity model for high reynolds number turbulent flows. *Computers & Fluids* **24** (3), 227–238. doi: 10.1016/0045-7950(94)00032-T.
- Sindall, R., Bridgeman, J. & Carliell-Marquet, C. 2013 Velocity gradient as a tool to characterise the link between mixing and biogas production in anaerobic waste digesters. *Water Science & Technology* **67** (12), 2800–2806. doi: 10.2166/wst.2013.206.
- Singh, B., Szamosi, Z. & Siménfalvi, Z. 2019 State of the art on mixing in an anaerobic digester: a review. *Renewable Energy* **141**, 922–936. doi: 10.1016/j.renene.2019.04.072.
- Singh, B., Szamosi, Z. & Siménfalvi, Z. 2020 Impact of mixing intensity and duration on biogas production in an anaerobic digester: a review. *Critical Reviews in Biotechnology*. In press, doi: 10.1080/07388551.2020.1731413.
- Stoppiello, M. G., Lofrano, G., Carotenuto, M., Viccione, G., Guarnaccia, C. & Cascini, L. 2020 A comparative assessment of analytical fate and transport models of organic contaminants in unsaturated soils. *Sustainability* **12**, 1–24, 2949. doi: 10.3390/su12072949.
- Subramanian, B., Miot, A., Jones, B., Klibert, C. & Pagilla, K. R. 2015 A full-scale study of mixing and foaming in egg-shaped anaerobic digesters. *Bioresource Technology* **192**, 461–470. doi: 10.1016/j.biortech.2015.06.023.
- Tang, J. 2009 *Comparison of Dairy Manure Anaerobic Digestion Performance in Gas-Lift and Bubble Column Digesters*. Master of Science Thesis, Virginia Polytechnic Institute and State University, Blacksburg, VA, USA.
- Tchobanoglous, G., Stensel, H. D., Tsuchihashi, R., Burton, F. L. & Abu-Orf, M. 2014 *Wastewater Engineering: Treatment and Resource Recovery*. McGraw-Hill Education, New York, NY, USA.
- Teixeira, E. C. & Do Nascimento Siqueira, R. 2008 Performance assessment of hydraulic efficiency indexes. *Journal of Environmental Engineering* **134** (10), 851–859. ASCE. doi: 10.1061/(ASCE)0733-9372(2008)134:10(851).
- Terashima, M., Goel, R., Komatsu, K., Yasui, H., Takahashi, H., Li, Y. & Noike, T. 2009 CFD simulation of mixing in anaerobic digesters. *Bioresource Technology* **100**, 2228–2233. doi: 10.1016/j.biortech.2008.07.069.
- Torotwa, I. & Ji, C. 2018 A study of the mixing performance of different impeller designs in stirred vessels using computational fluid dynamics. *Designs* **2** (1), 10. doi: 10.3390/designs2010010.
- Vesvikar, M. S. & Al-Dahhn, M. 2005 Flow pattern visualization in a mimic anaerobic digester using CFD. *Biotechnology and Bioengineering* **89**, 719–732. doi: 10.1002/bit.20388.
- Viccione, G., Zarra, T., Giuliani, S., Naddeo, V. & Belgiorno, V. 2012 Performance study of e-nose measurement chamber for environmental odour monitoring. *Chemical Engineering Transactions* **30**, 109–114. doi: 10.3303/CET1230019.
- Wang, J., Xue, Q., Guo, T., Mei, Z., Long, E., Wen, Q., Huang, W., Luo, T. & Huang, R. 2018 A review on CFD simulating method for biogas fermentation material fluid. *Renewable and Sustainable Energy Reviews* **97**, 64–73. doi: 10.1016/j.rser.2018.08.029.
- Wang, H., Larson, R. A., Borchardt, M. & Spencer, S. 2019 Effect of mixing duration on biogas production and methanogen distribution in an anaerobic digester. *Environmental Technology*. In press, doi:10.1080/09593330.2019.1621951.
- Wu, B. 2010 CFD simulation of gas mixing in egg-shaped anaerobic digester. *Water Research* **44**, 1507–1519. doi: 10.1016/j.watres.2009.10.040.

- Wu, B. 2011 CFD investigation of turbulence models for mechanical agitation of non-Newtonian fluids in anaerobic digesters. *Water Research* **45** (5), 2082–2094.
- Wu, B. 2012 Large eddy simulation of mechanical mixing in anaerobic digesters. *Biotechnology and Bioengineering* **109** (3), 804–812. doi: 10.1002/bit.24345.
- Wu, B. 2014 CFD simulation of gas mixing in anaerobic digesters. *Computers and Electronics in Agriculture* **109**, 278–286. doi: 10.1016/j.compag.2014.10.007.
- Wu, B. & Chen, S. 2008 CFD simulation of non-Newtonian fluid flow in anaerobic digesters. *Biotechnology and Bioengineering* **99**, 700–711. doi: 10.1002/bit.21613.
- Zare, A. D., Saray, R. K., Mirmasoumi, S. & Bahlouli, K. 2019 Optimization strategies for mixing ratio of biogas and natural gas co-firing in a cogeneration of heat and power cycle. *Energy* **181**, 635–644. doi: 10.1016/j.energy.2019.05.182.

First received 6 June 2019; accepted in revised form 11 May 2020. Available online 18 May 2020